JOURNAL OF AIRCRAFT
Vol. 39, No. 6, November–December 2002

From Water Tunnel to Poststall Flight Simulation: The F/A-18 Investigation

Martin E. Beyers
Institute for Aerospace Research, Ottawa, Ontario K1A 0R6, Canada

Introduction

THE prediction of poststall maneuvers and departure characteristics of high-performance aircraft continues to be challenging,[1,2] due, in particular, to the highly three-dimensional nature of the motions and aerodynamic responses.[3] A case in point is the F/A-18 aircraft (Fig. 1), which has experienced departures from controlled flight, typically involving large sideslip excursions with attendant high body-axes rate variations leading to high angles of attack α (Ref. 4). The lateral–directional departure susceptibility of the F/A-18 provided part of the motivation within the NASA High-Alpha Technology Program for the improvement of high-alpha predictions based on ground testing.[5] The gyrations and responses experienced on departure are intrinsically nonplanar, that is, involving arbitrary rotations not aligned with the principal axes of the aircraft.[3] When the flight mechanical deficiencies of an F/A-18 simulation were identified, a Canadian program was undertaken to enhance simulator fidelity.[6] The areas in which the airframe model could be improved included the poststall aerodynamic database, the multivariable table lookup architecture, and the aerodynamic model. The present paper focuses on the improvements to the database. The shortcomings of the poststall aerodynamic database were attributed largely to facility interference[7,8] and scaling effects[9,10] not accounted for and gaps in the parameter space covered. The original rotary database for F/A-18 was generated in the NASA Langley Research Center Spin Tunnel.[11] The F/A-18 poststall maneuvering aerodynamics is dominated by forebody/leading edge extension (LEX) vortex interactions at moderately high angles of attack ($30 < \alpha < 55$ deg) and forebody flow separation asymmetry at high alpha ($\alpha > 55$ deg). In the light of the sensitivity of the vortex interactions to sideslip angle β (Ref. 12), it was deemed necessary to generate a more detailed rotary database to define the associated relationships over a large sideslip range.

When the advantages of the water-tunnel approach were considered, it seemed appropriate to use this ground-test methodology to generate supplementary data. The orbital platform rotary balance system (OPLEC)[13] at the Institute for Aerospace Research (IAR) water tunnel, a diagnostic tool for studying support interference[7,8] and unsteady wall interference,[14] was subsequently used in high-resolution tests as well as diagnostic experiments[15–18] on the baseline F/A-18. A thorough understanding of scale effects on vortex breakdown and interaction characteristics was seen as a prerequisite to extrapolation to full scale of water-tunnel dynamic data. Unlike the case with delta wings, the F/A-18 vortex breakdown characteristics at low Reynolds number *Re* have shown remarkable agreement with low Mach number flight test results.[6,19,20] A favorable comparison[21] was also made under dynamic conditions of wing rock.[20,22] However, early experiments[12] had revealed discrepancies between lateral–directional aerodynamic results at different test scales. In reality, differences between flow separation characteristics on bodies of revolution at laminar, transitional, and turbulent Reynolds numbers[23,24] show that the correspondence between subscale and flight-test results cannot be universal. Because of the very different side force distributions on the F/A-18 forebody at laminar and fully turbulent conditions, the extrapolation of laminar water-tunnel results to full-scale conditions could only be valid under a rather special set of circumstances. The question to be answered is whether the favorable wing rock comparison[21] was fortuitous or whether there is a useful part of the poststall maneuvering envelope within which the laminar water-tunnel results could be exploited in flight predictions.

This paper surveys the experimental efforts of defining the nonplanar aerodynamic characteristics of the F/A-18, consolidating the database and, in particular, confronting the issues of scaling and the effects of the dynamic test environment.

Background

Although a simple six-degree-of-freedom (DOF) model of the unsteady aerodynamics of aircraft maneuvering flight is not likely to be developed any time soon,[2] significant improvements to the quasi-steady models in use[1] could lessen the reliance on empirical adjustments to the model that have become commonplace.[25] Because the linearized model breaks down in the presence of aerodynamic bifurcation,[26,27] the boundaries of the regions of its validity are an important part of the information needed for the implementation of the database in the 6-DOF simulation. To enhance the steady-state model, the relationships between the aerodynamic responses that exist for the F/A-18 aircraft under steady nonplanar motion conditions were analyzed, and similarity parameters derived from flow physics considerations were introduced.[6]

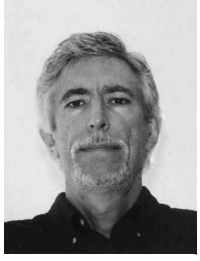

Martin Beyers is a Principal Research Officer at the National Research Council Canada. As Head of the Aircraft Aerodynamics Group, he was responsible for research programs on civil and combat aircraft, and aircraft icing, until 2001. Since 1965, his principal research focus has been in maneuvering aerodynamics, unsteady aerodynamics, and free-flight dynamics, and he has published 140 articles in the related fields. He has introduced new concepts for dynamic testing and modeling of high-alpha flight vehicle aerodynamics. He has a Ph.D. from Witwatersrand University. He was an Associate Editor of the *Journal of Aircraft* for six years and has served on several international panels, including two AIAA technical committees. He is a fellow of the Canadian Aeronautics and Space Institute and a Senior Member of AIAA.

Presented as Paper 2002-0699 at the AIAA 40th Aerospace Sciences Meeting and Exhibit, Reno, NV, 14 January 2002; received 26 March 2002; revision received 13 May 2002; accepted for publication 13 May 2002.

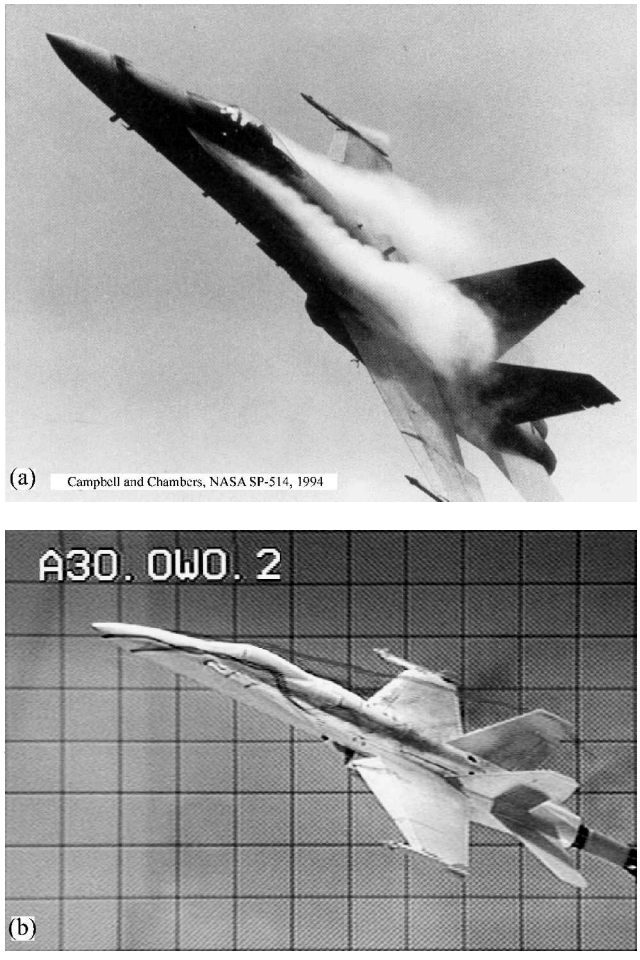

Fig. 1 F/A-18 at full scale and model scale: a) CF-18 at high alpha and b) scale model at high rotation rate.

Predictions in the poststall flight regime rely heavily on the experimental knowledge base.[3] The poststall database of the F/A-18 aircraft (Fig. 1) is arguably the most extensive for any existing fighter aircraft. Yet there are still gaps in the single-DOF dynamic data that restrict the fidelity of any nonplanar motion simulation. The use of experimental dynamic data in flight dynamic predictions introduces a related set of problems, including those of database structure,[6] effects of experimental conditions,[7–9,14] and extrapolation to full scale.[3,9]

The F/A-18 rotary data were obtained from published[11] and unpublished tests in the NASA Langley Research Center Spin Tunnel, the NASA Ames Research Center 7 × 10 Foot Wind Tunnel,[28] and in water tunnels, at Eidetics Corporation[29] and at IAR.[15–17] The sources of static lateral–directional aerodynamic data for the baseline F/A-18 at asymmetric test conditions are found in Refs. 30–33, and flow visualization data are provided in Refs. 15, 16, 31, 32, and 34–36. Flight-test data on the High-Alpha Research Vehicle (HARV)[19,20,34] were obtained at NASA Dryden Flight Research Center.

IAR Experimental Program

Test Equipment

The 1/72-scale model of the F/A-18 used in the IAR experiments[15] (Fig. 2) incorporates a 34-deg leading-edge flap deflection δ_{LE} and neutral control surface settings and featured flow-through engine inlets. On either side close to the nose apex, the LEX apex and LEX/wing junction, 12 dye ports were arranged, as shown in Fig. 3. The model was mounted on a five-component submersible balance with the rotation center at 25% mean aerodynamic chord (MAC). Details of the measurement and data acquisition systems can be found in Refs. 15–17. For force measurements and flow visualization, the Reynolds number based on MAC *Re* was 1.78×10^4 and 6.46×10^3, respectively.

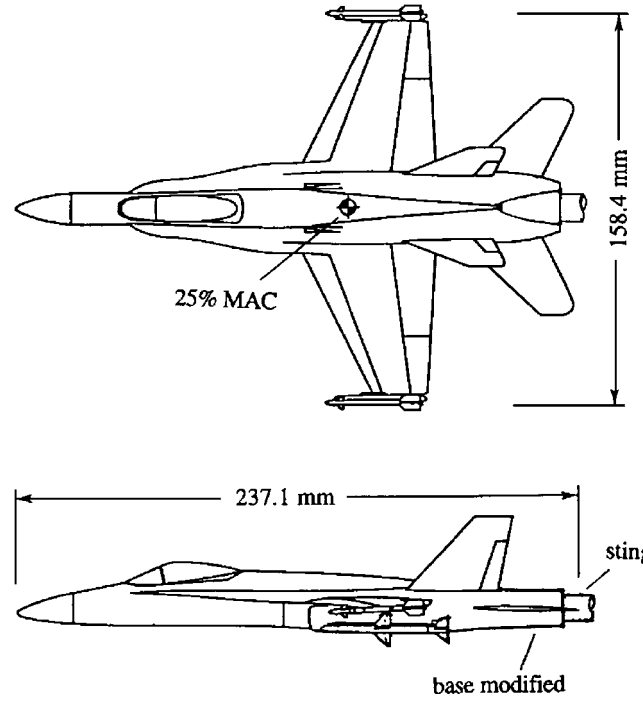

Fig. 2 F/A-18 1/72-scale model.

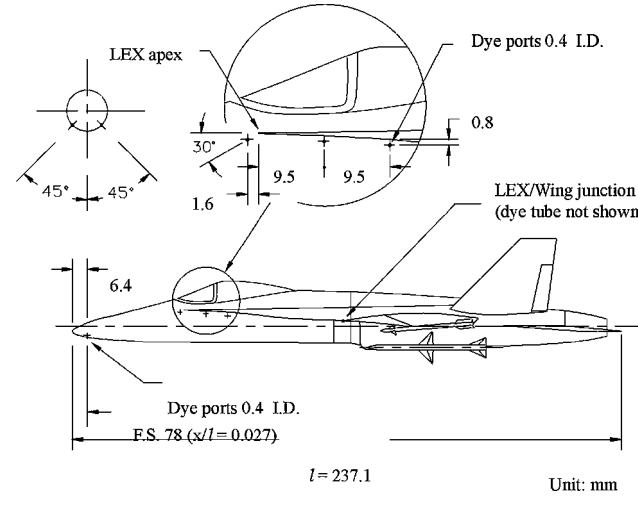

Fig. 3 Dye port locations on model.

An advanced orbital platform apparatus[13] (Fig. 4) was used for rotary experiments in the IAR 0.38×0.51 m Water Tunnel. The model is mounted on a sting attached to an annular platform, riding on the outer surface of a stationary, cylindrical test section insert (Fig. 5). With the absence of the conventional shaft-mounted C-strut or arm, the aerodynamic interference is minimal because the strong-interaction support interference[3] is eliminated. The aft-mounted model is set at a pitch angle σ on a short circular sector, which is carried on a yoke attached to the support arm. An indexing spacer between the sting and the yoke is used to set the bank angle ϕ at discrete values at intervals of 2.5 deg in the range $|\phi| \leq 50$ deg. The relationship between the angles α, β and σ, ϕ is $\alpha = \tan^{-1}(\tan\sigma \cos\phi)$ and $\beta = \sin^{-1}(\sin\sigma \sin\phi)$. To investigate support interference at high alpha, replicas of the support systems used in conventional rotary rigs are mounted on the orbital platform.[15,16]

Representative Results

Figure 6 shows the IAR lateral–directional rotary characteristics[15] obtained at IAR in the range of symmetric crossflow separation at

Fig. 4 Rear view of orbital platform apparatus.

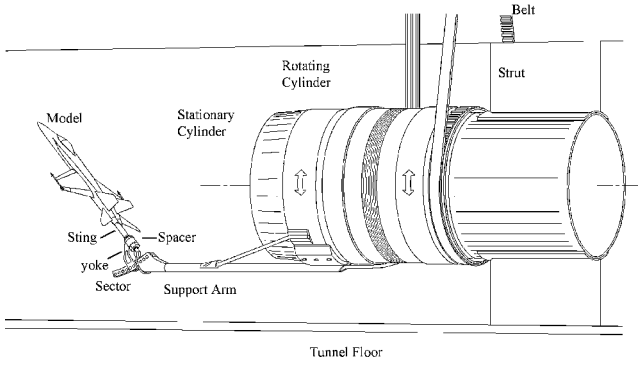

Fig. 5 Schematic layout of orbital platform apparatus.

$\beta = 0$ and $|\bar{\Omega}| \leq 0.3$, where $\bar{\Omega} = \Omega b/2U_\infty$ is the dimensionless coning rate. Flow visualization revealed the existence of three critical points, two associated with LEX vortex breakdown crossing the LEX–wing junction at $\alpha \cong 28$ deg (slope changes at this condition shown in Fig. 6) and reaching the LEX apex at $\alpha \cong 50$ deg and the third associated with the onset of asymmetric crossflow separation on the forebody at $\alpha \cong 55$ deg. At this point, the responses become discontinuous, with steady-state hysteresis occurring in the range $57.5 \leq \alpha \leq 67.5$ deg. A well-defined coning-hysteresis loop exists at $\alpha = 60$ deg (Fig. 7). At intermediate α, a variety of complex forebody/LEX vortex interactions occur, ranging from co rotating vortex interactions before LEX vortex breakdown (Fig. 8b) to vortex cross interactions (Fig. 8a). For the latter type, the attached forebody vortex crosses over, under the influence of the sidewash generated in the nonplanar, curved flowfield. The interaction then switches from the retreating to the advancing side as $|\bar{\Omega}|$ increases, reducing the upwash on the advancing side. The coning-induced positive camber delays vortex breakdown on that side. An interaction occurring between the leeward body vortex and leeward burst LEX vortex is referred to as a "weak" interaction. As the rotation rate increased above a threshold rotation rate $\bar{\Omega}_T$ (Ref. 37) the interaction occurred before breakdown, termed a "strong" interaction (Figs. 8a and 9).

In the nonlinear range $57.5 \leq \alpha \leq 67.5$ deg, for motions initiated at a dimensionless coning rate $\bar{\Omega}_S$ outside the hysteresis loop (Fig. 7), the behavior is very steady, but when the motion starts within the loop, that is, in the range $|\bar{\Omega}_S| < |\bar{\Omega}_T|$, a high degree of

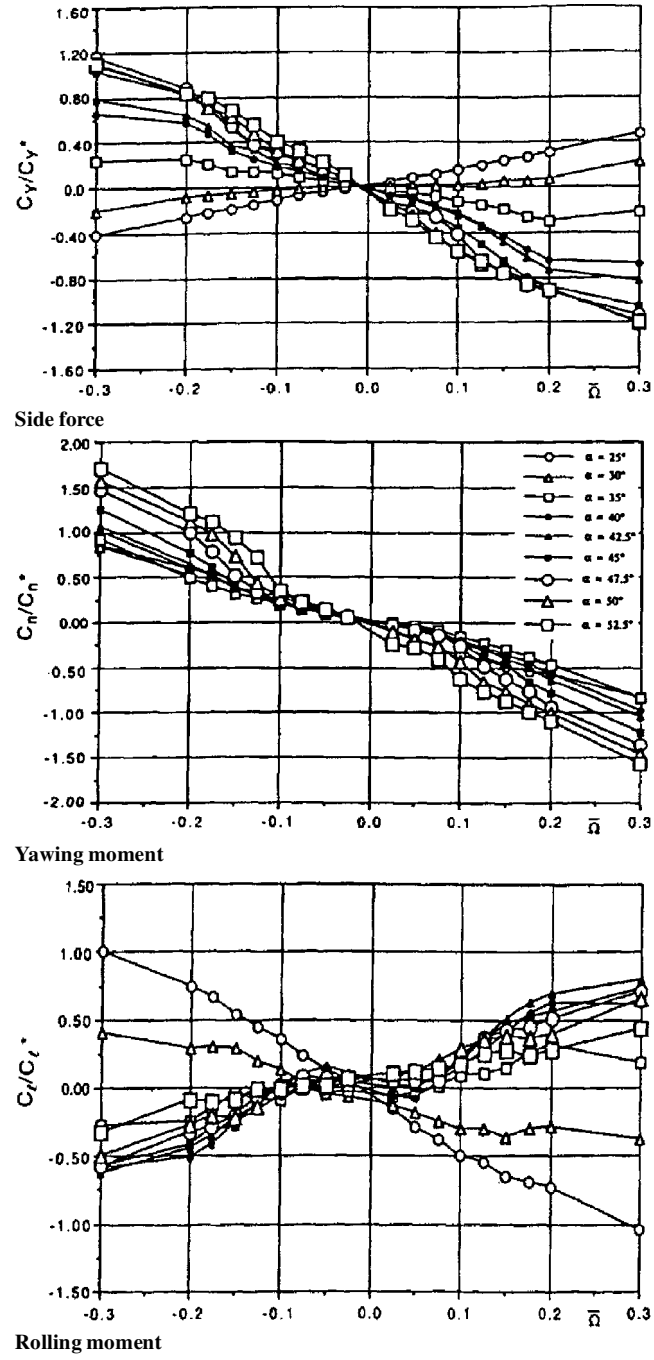

Fig. 6 Effect of rotation rate on lateral–directional aerodynamic characteristics, $\beta = 0$.

unsteadiness exists, which signals the occurrence of apparently random bifurcations.[17] Under these conditions, when the threshold $\bar{\Omega}_T$ was never crossed,[37] a high degree of sensitivity to support interference was observed (Fig. 10).[38] In the vortex interaction range, no steady-state hysteresis was detected,[17] but the existence of a dorsal support affects the forebody/LEX vortex interactions, influencing the spanwise flow over the associated wing-half, and affecting the magnitude of the rolling moment.[15] At certain conditions, the influence of the support caused the interaction to switch from the retreating to the advancing sides, accompanied by a change in sign of the rolling moment C_l.

Analysis of a large number of video flow visualization records yielded the characterization of the vortex interactions over the α–$\bar{\Omega}$ range, as summarized in Fig. 11 (Ref. 18). At low $\bar{\Omega}$ and $\alpha \leq 42.5$ deg, essentially symmetric forebody vortex shedding occurred. Beyond the range $-0.05 \leq \bar{\Omega} \leq 0$, the coning rate dominates, and the forebody vortex on the advancing side becomes detached

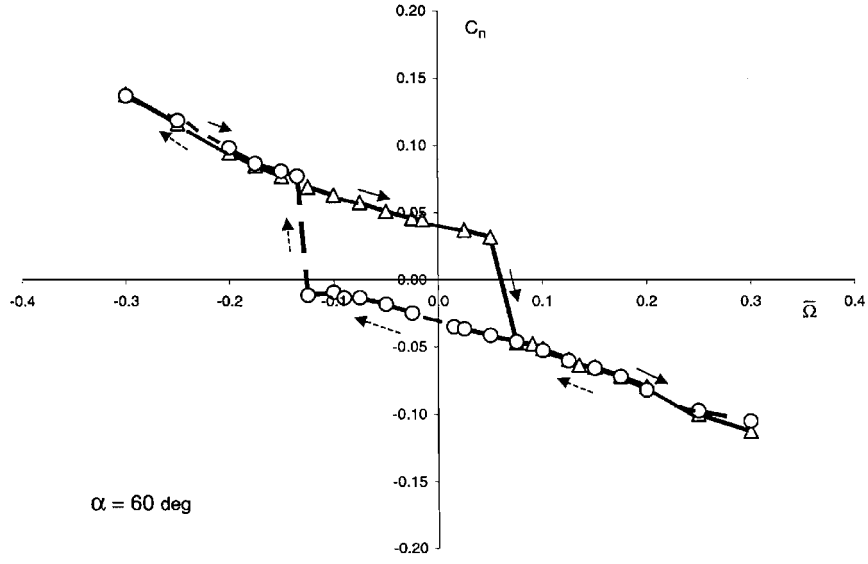

Fig. 7 Steady-state coning hysteresis at $\alpha = 60$ deg.

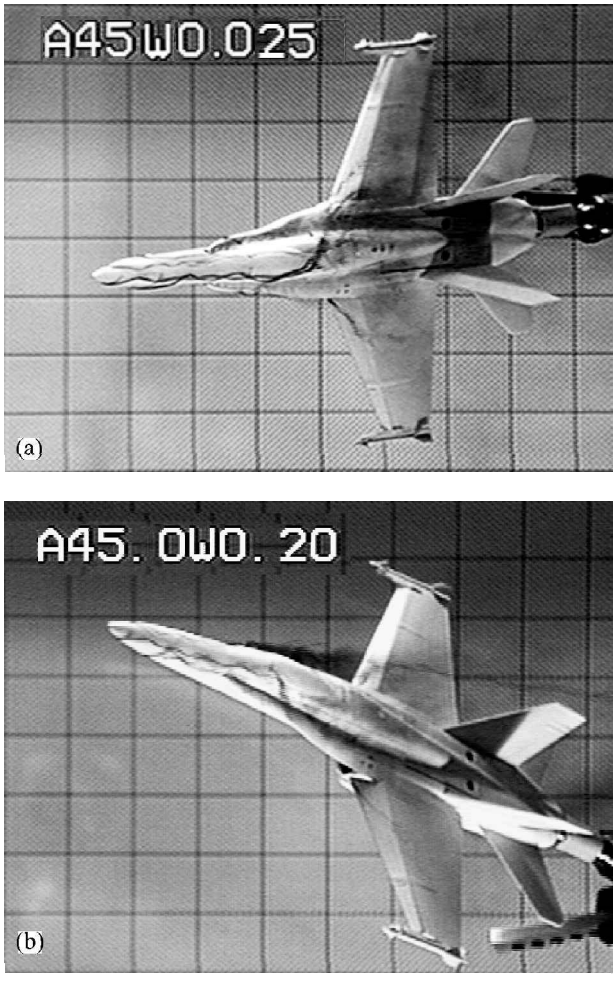

Fig. 8 Vortex interactions on rotating model at $\alpha = 45$ deg: a) cross-vortex interaction and b) strong interaction.

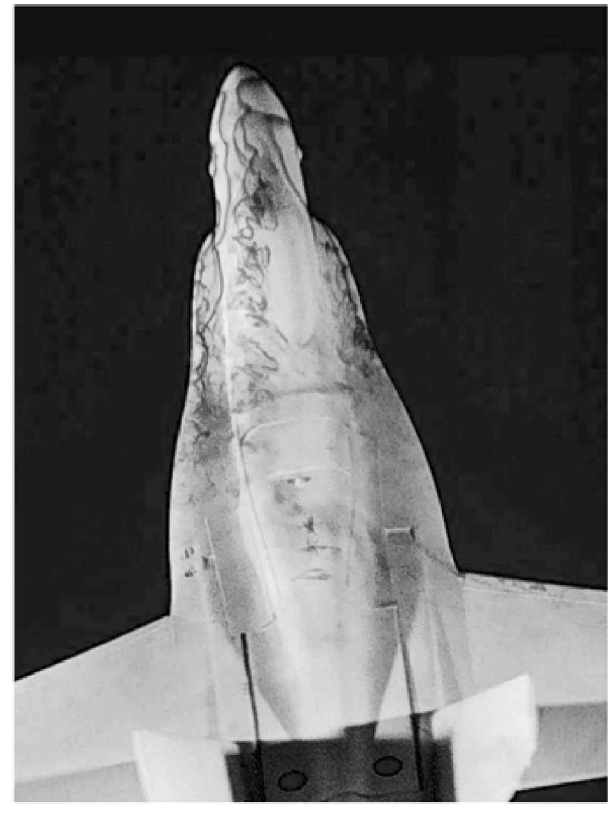

Fig. 9 Strong vortex interaction at $\alpha = 40$ deg and $\bar{\Omega} = 0.2$ (rear view).

from the surface through the coning-induced LEX upwash bubble effect,[6] resisted by the moving-wall effect on the forebody.[39] At substantial rotation rates in the range $45 \leq \alpha \leq 55$ deg, vortex cross-interaction occurs. The strong interactions occurred at $\alpha \leq 47.5$ deg and $|\bar{\Omega}| \geq 0.15$. The domains of vortex interaction are separated by regions of unsteadiness. Asymmetries in the boundaries of these regions are attributed to model geometric asymmetry and possible tunnel flow nonuniformity.

Sideslip Effects on Forebody/LEX Vortex Interaction

At $\beta \neq 0$, the flowfield interactions and, in particular, LEX vortex breakdown is affected by the changes in effective leading-edge sweep angle on the two sides.[6,17] In rotary motion, the flowfield interactions are determined by the overall velocity distribution resulting from the combination of body-axes sideslip and coning-induced local sideslip effects. With different combinations of $\bar{\Omega}$ and ϕ, the sideslip effect on forebody/LEX vortex interaction might be augmented or canceled out. At $\alpha \leq 35$ deg, $C_l(\beta)$ becomes highly nonlinear with β as LEX vortex breakdown moves back onto the retreating wing-half with increasing β. As illustrated for $\sigma = 45$ deg (Fig. 12), the aerodynamics are nonlinear, with anti-symmetric trends in the rolling moment over the vortex interaction range.[17] At $\sigma = 40$ deg and $\phi = 0$ ($\beta = 0$), C_l has an inflection

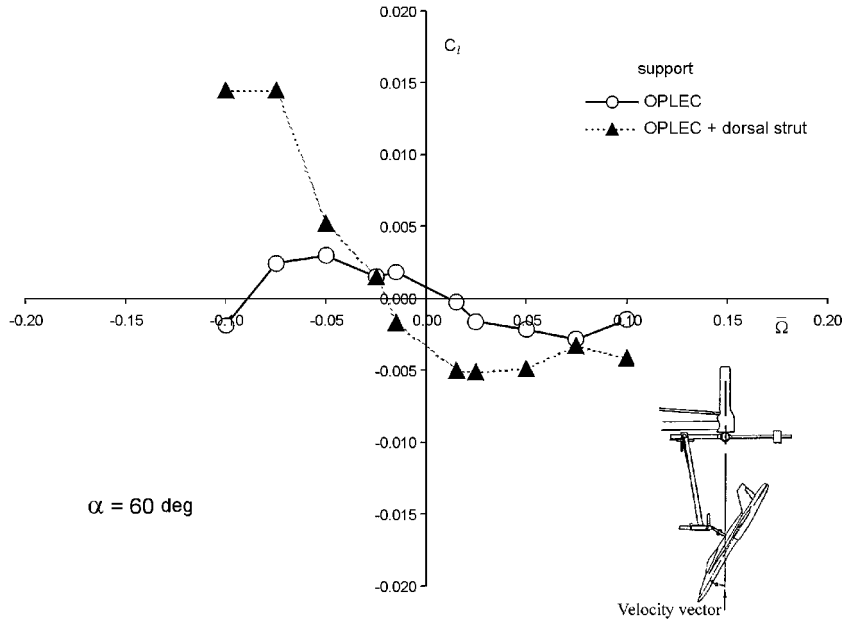

Fig. 10 Effect of dorsal strut in water-tunnel test for $|\bar{\Omega}_s| < |\bar{\Omega}_T|$.

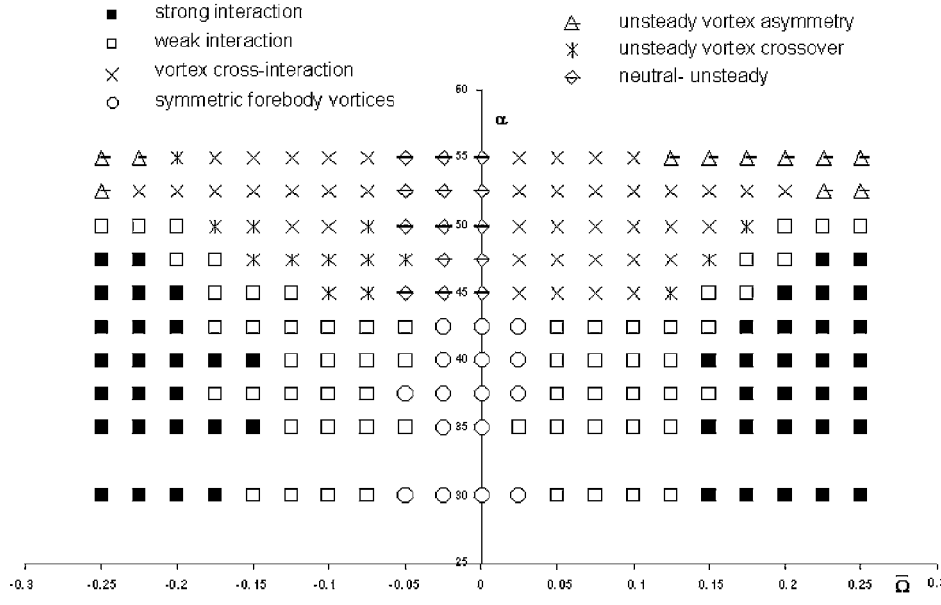

Fig. 11 Map of forebody/LEX vortex interaction conditions.

point at $\bar{\Omega} = 0$, corresponding to a near-symmetric vortex system (Fig. 13a). At $\Omega \geq 0.1$, C_l increases with increasing $\bar{\Omega}$, as a result of the leeside strong vortex interaction due to coning motion (Fig. 13b). However, when $\phi > 0$, for instance, $\phi = 15$ deg ($\alpha \approx 40$ deg and $\beta \approx 10$ deg), the inflection point is shifted to $\bar{\Omega} < 0$ (Fig. 13d), where the two vortex systems are again "symmetric" at $\bar{\Omega} = -0.1$. When a vortex cross interaction occurred at $\bar{\Omega} = -0.2$ (Fig. 13c), a positive C_l increment resulted.

Intertechnique Comparison

A natural question to be answered is to what extent can the laminar water tunnel results be extrapolated to full-scale conditions. If indeed feasible, the new data would constitute a useful extension of the nonplanar database on the baseline configuration. Thus, dealing with the scaling issues became a priority.

LEX Vortex Breakdown

An obvious starting point seemed to be the documented insensitivity to Reynolds number of the LEX vortex breakdown (Fig. 14) on the F/A-18 aircraft configuration over the complete Reynolds number range from water-tunnel tests to full-scale flight,[6,18,19] which contrasts sharply with the high sensitivity displayed by vortex breakdown on delta-wing configurations.[40] The observed effect of increasing Reynolds number on pure delta wings[40–42] (Fig. 15), as well as on a combat aircraft model with extensive LEX surfaces,[43] was to promote vortex breakdown.

It has been demonstrated in the case of a delta-wing–body[44] that the body-induced upwash distribution along the wing leading edge generates a negative wing-camber effect that promotes vortex breakdown.[45] The presence of a fuselage will promote vortex breakdown to occur much earlier than for an isolated wing. Similarly, in the case of the F/A-18 configuration (Fig. 16), the body radius is approximately constant over the initial LEX extent, and the body-induced negative camber effect along the leading edge would promote vortex breakdown in the absence of other effects. When considering the flow conditions close to the fuselage, the boundary layer has considerable influence, creating, in effect, a viscous fairing. The viscous fairing effects on the bottom half of the fuselage would increase the effective body radius, thereby generating a negative body-induced camber effect and associated promotion of vortex breakdown that is of larger magnitude for laminar than

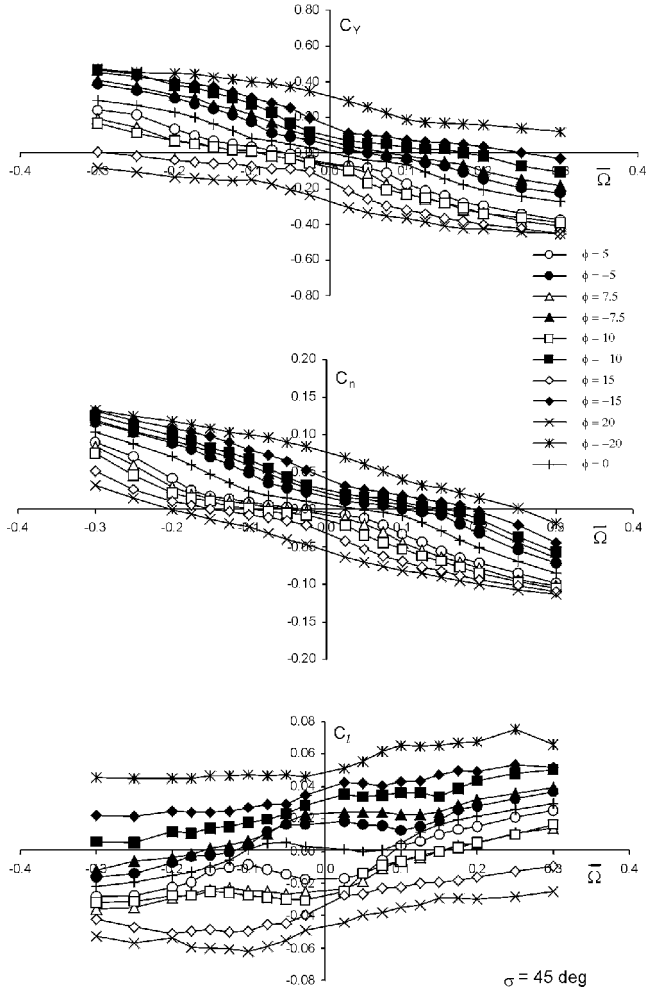

Fig. 12 Lateral–directional aerodynamic characteristics at $\sigma = 45$ deg and $|\phi| \leq 20$ deg.

for turbulent flow conditions.[46,47] Looking at the gothic planform of the forward portion of the LEX (Fig. 16), one can see how the rapidly increasing span near the LEX apex could have made the initial LEX vortex development rather insensitive to the difference between body-induced upwash for laminar and turbulent flow conditions. In addition, the viscous fairing effect on the longitudinal body geometry (Fig. 17) would be to generate body conicity, thereby reducing the LEX wing area and increasing the effective leading-edge sweep. This could have delayed the LEX vortex breakdown,[48] compensating for the breakdown-promoting effect of the increased body-induced negative camber caused by the effective increase in body radius. These two viscous fairing effects apparently more or less canceled each other, accounting for the observed insensitivity of LEX vortex breakdown to the Reynolds number (Fig. 14).

Vortex Interaction Characteristics

On the F/A-18 HARV, wing rock observed in flight tests was associated with forebody/LEX vortex interactions at $\alpha \cong 45$ deg (Refs. 20 and 49). Subsequent laminar subscale tests[21] showed good agreement with flight tests (Fig. 18),[20] even after accounting for the bearing friction in the test.[49] This indicated that both the vortex interaction and vortex breakdown characteristics had to have been simulated correctly. In contrast, interactions of corotating vortices on double delta wings have been found to be sensitive to Reynolds number.[50–52] The effect of Reynolds number on the vortex interaction location is similar to that on vortex breakdown, with the interaction point moving upstream as Reynolds number Re is increased.

Comparisons of flow visualization in water-tunnel tests and in flight,[18] allowing for differences in the viewing angle, indicate that the vortex interactions are quite similar at angles of sideslip approaching zero for $\alpha = 40$ (Fig. 19), 42.5, and 45 deg. Comparisons between water-tunnel and flight-test results at $\beta \neq 0$ are difficult because the prevalence of wing rock makes it all but impossible to stabilize the aircraft at asymmetric flight conditions. Nevertheless, the degree of similarity between wind tunnel and flight is encouraging.[18] Good agreement was obtained between measurements of the vortex interaction point in water tunnels[16,19] and in flight[34] (Fig. 20).

A comparison of the lateral–directional aerodynamic characteristics would give an idea of the degree of correspondence of the global loads over the β range. The results at $\alpha = 40$ deg from several facilities, including water tunnel and wind tunnels at various Reynolds numbers and model scales, are compared in Fig. 21. The α, β values corresponding to discrete σ, ϕ combinations were approximate, within ± 0.7 deg of the corresponding plotted values. The C_Y data from the different facilities agreed reasonably well, except in the case of the Eidetics data.[33] This is attributed to wall interference effects, which were not corrected for.[33] On the whole, the yawing moment shows good agreement. Different slopes of $C_l(\beta)$ at $\beta \neq 0$ exist between the water tunnel results (from IAR[15] and Eidetics[33]) and low Reynolds number wind-tunnel results (from the NASA Langley Research Center Spin Tunnel[11] and the U.S. Navy David Taylor Research Center (DTRC) 7×10 Foot Wind Tunnel[31]), whereas the high Reynolds number results from the NASA Ames Research Center full-scale wind tunnel[30] differed from both groups. However, the slope $C_{l\beta}$ of the full-scale data agrees with that of the IAR data at $\beta \leq -3$ deg and $\beta \geq 3$ deg. The nonlinearity at $|\beta| < 5$ deg is likely due to the stronger vortex interactions at lower laminar Reynolds numbers. The discrepancies between the IAR and Eidetics C_l data again are attributed to the larger wall interference effects in the latter case. The smaller slope in the DTRC data is attributed to the documented use of boundary-layer trips.[31]

The larger slope of $C_l(\beta)$ that exists for small β in Fig. 21 has to be explained. At $30 < \alpha < 50$ deg, the aerodynamic loading is largely generated by attached flow on the windward lifting surfaces and vortex-induced suction on the leeward surfaces of the LEX-wing configuration. Because LEX vortex breakdown reaches the wing apex at $\alpha \cong 28$ deg, the suction generated on the wings derives primarily from the spiral flow[53] downstream of breakdown. The location and nature of forebody/LEX vortex interactions have a profound effect on the wing loading and, as shown by water-tunnel flow visualization,[16] can influence the spanwise flow on the wing-half affected. The weak interactions tend to be unsteady, and the strong interactions generally steady. Both types have been observed in flight tests of HARV[20,34] at $\beta \cong 0$ and $|\beta| > 5$ deg, respectively. Under these conditions, the agreement between water-tunnel and flight results at $0.2 < M < 0.4$ is good, indicating the overall scale effects are not acute.

It appears that at $|\beta| < 5$ deg the viscous fairing effects postulated in Ref. 40 play a role. The body-induced negative camber[44–46] is augmented by the viscous fairing effect of the thickened boundary layer on the fuselage, more so at the laminar Reynolds numbers in the water tunnel. This would promote vortex breakdown. Also, as a result of the viscous fairing effect of producing body conicity, the effective leading-edge sweep on the leeward LEX is increased. The two effects largely cancel each other at zero sideslip.[40] At small $|\beta|$, the asymmetry in the attachment line will tend to accentuate the effect of body conicity on the leeward LEX, through the increased thickness of the viscous region (Fig. 22). This associated increased sweep could have produced a delay of vortex breakdown, but with reduction in leading-edge vortex strength and, therefore, vortex-induced suction, giving $\Delta C_l < 0$.

At large β ($|\beta| \geq 5$ deg), the leeward primary separation is located near an azimuth $|\varphi| < 70$ deg, and viscous fairing effects become ineffective. With the reduction in leading-edge sweep, the leading-edge vortex strength is increased, resulting in an increase in the extent of the spanwise flow on the leeward wing-half. The increased suction loading that results is less sensitive to Reynolds number, with $\Delta C_l > 0$ for $\beta \gg 0$ (Fig. 22), returning the trend to the moderately stabilizing slope existing at full-scale conditions.

The conclusion is that, at the Reynolds number of the water tunnel, vortex interactions are highly sensitive to sideslip angle or

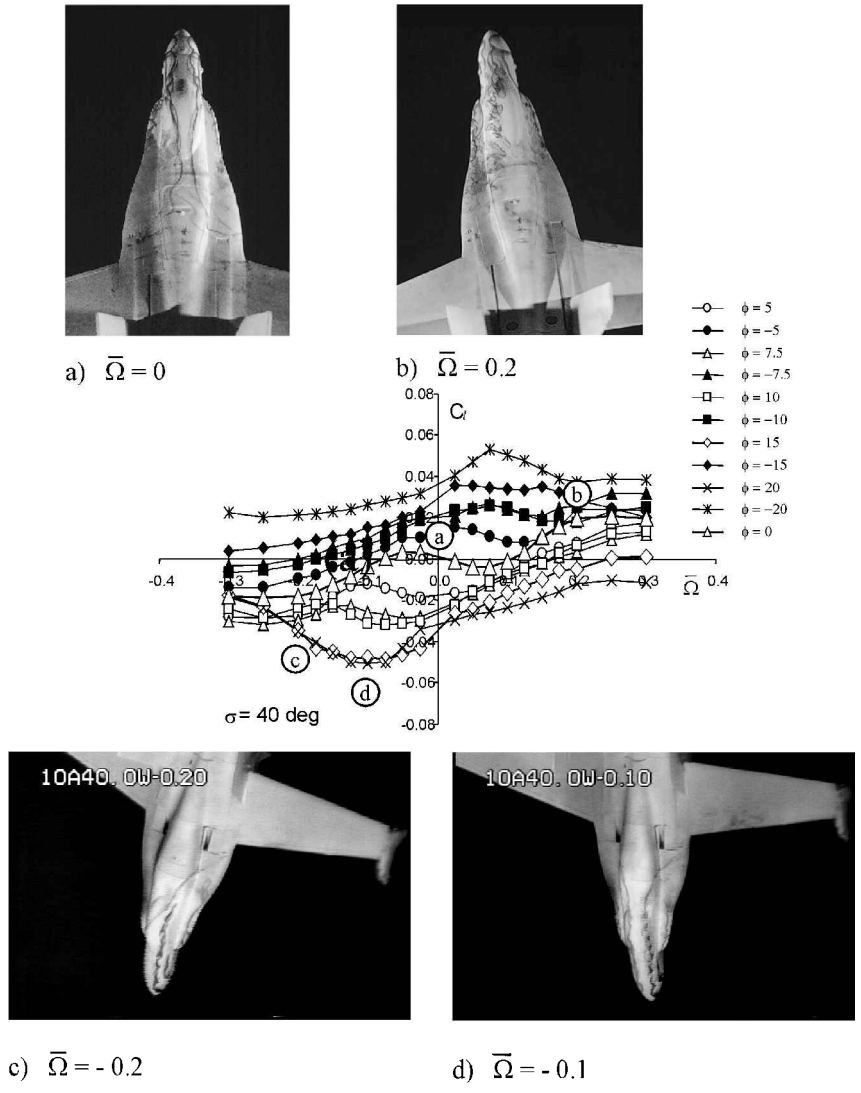

Fig. 13 Sideslip effects on forebody/LEX vortex interaction in rotation at $\sigma = 40$ deg.

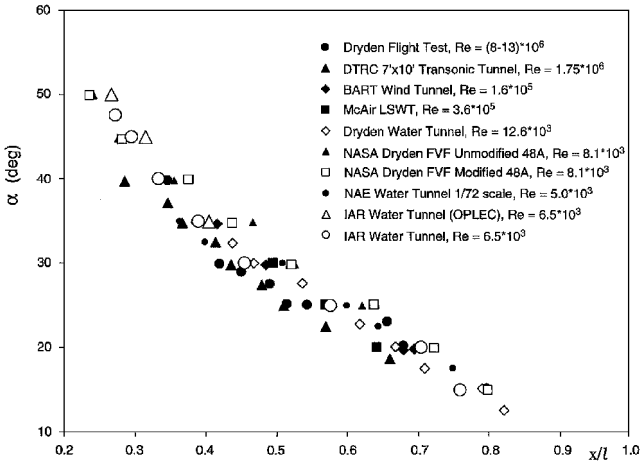

Fig. 14 Correlation of F/A-18 LEX vortex breakdown position.[15,16,31,32,34–36]

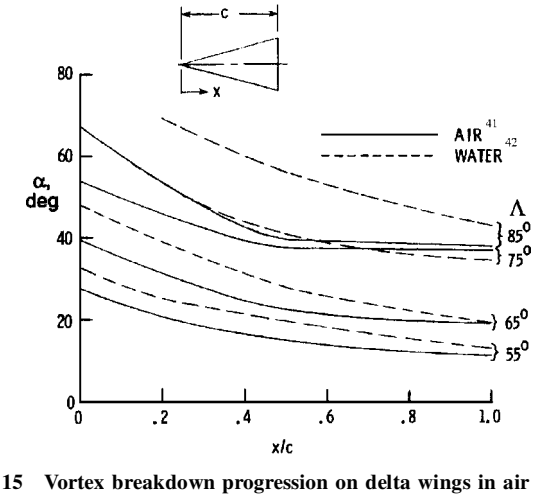

Fig. 15 Vortex breakdown progression on delta wings in air and in water.

coning-induced velocity distributions, but that the similarity between laminar and fully turbulent conditions that exists at $\beta \to 0$ and $\beta \geq 5$ deg does not extend to small finite β ($0 < |\beta| \leq 3$ deg).

Compressibility

The good agreement obtained between measurements of the vortex interaction location in water tunnels and in-flight (Fig. 20) poses the next question: How can the vortex interaction characteristics be similar when the relative vortex strengths have changed due to viscous fairing effects? For a constant chord length, the leading-edge vortex strength of slender delta wings decreases with increasing leading-edge sweep.[54] Thus, the effective increase of the LEX sweep near the apex, caused by viscous fairing effects at laminar conditions, will be accompanied by a reduction in LEX vortex strength. Downstream of the apex, the leading-edge vortex is

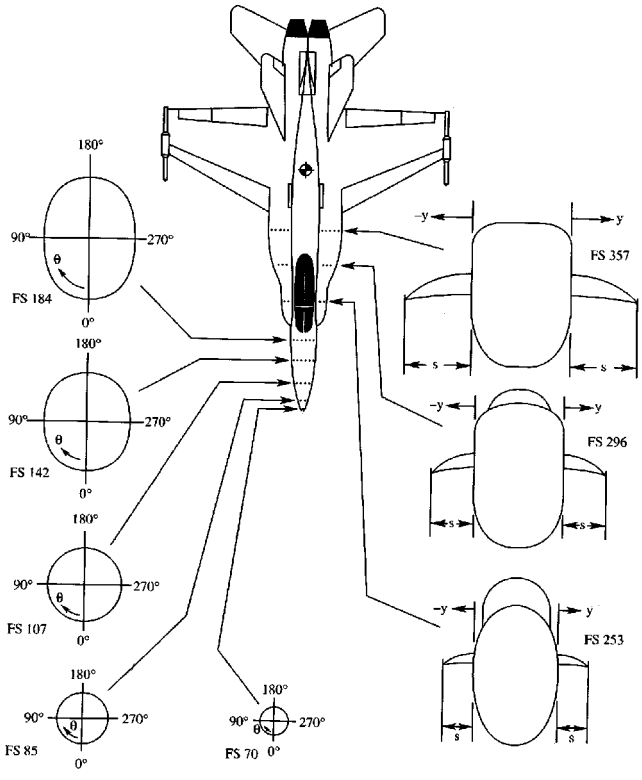

Ghaffari, NASA, TP-3478, 1994

Fig. 16 F/A-18 cross-sectional geometry.

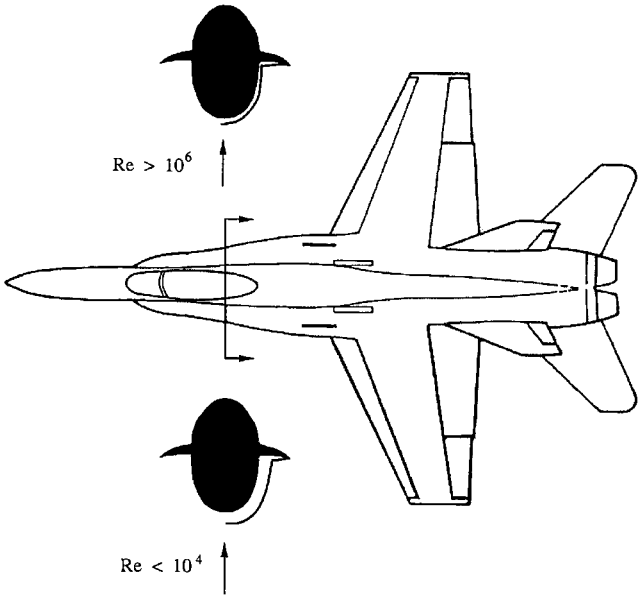

Fig. 17 Viscous fairing effects on F/A-18 model.

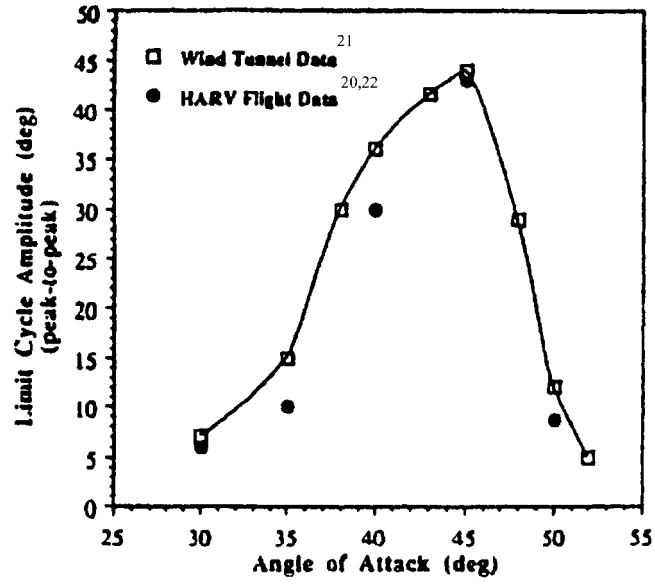

Fig. 18 Wing rock amplitude for F/A-18 measured in flight and in subscale tests.

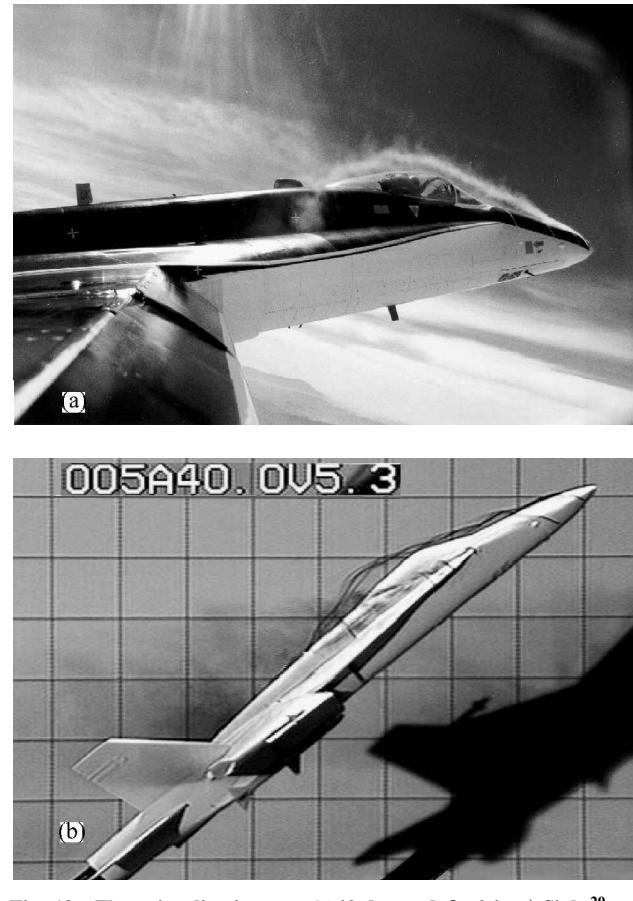

Fig. 19 Flow visualization at $\alpha \cong 40$ deg and $\beta = 0$ in a) flight[20] and b) water tunnel.[16]

apparently generated farther outboard along the gothic-leading-edge LEX segment, further reducing the vortex-induced loading on the LEX and delaying vortex interaction. In the flight tests, this effect was negligible. However, another factor was present, namely, compressibility.

The HARV flow visualization tests were conducted at Mach numbers between 0.2 and 0.4 (Ref. 19). The forebody flows are essentially free of compressibility effects in this range, as was to be expected, because the compressibility effects on an inclined circular cylinder are negligible[24] for $M_\infty \sin\alpha < 0.4$. On the other hand, as the Mach number is increased, the vortex-induced suction pressure on the LEX is reduced significantly.[55] The effects of Mach number on the LEX pressures were found to persist[56] to $M_\infty < 0.3$. The in-flight data at $\alpha = 31$ deg show that, even downstream of vortex breakdown, the suction pressures are influenced significantly by compressibility[55] (Fig. 23). This effect was also seen in the comparison[31] between data obtained on 6 and 16% scale models of F/A-18 at $Re = 1.0 \times 10^6$. Moreover, discrepancies between wind-tunnel data on 6% F/A-18 models at different Mach

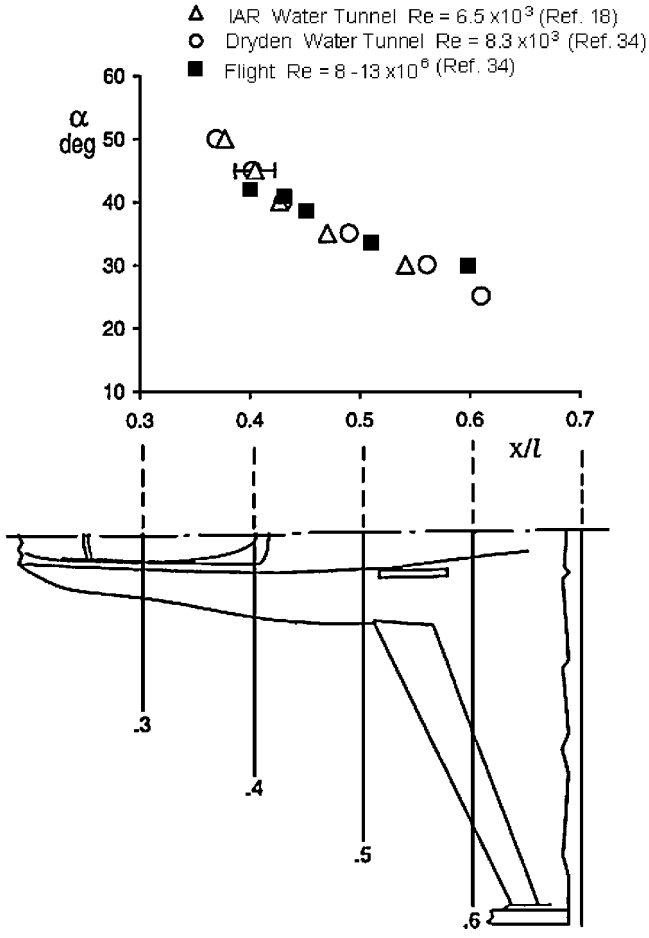

Fig. 20 Comparison between measurements of vortex interaction point in water tunnels and in flight.

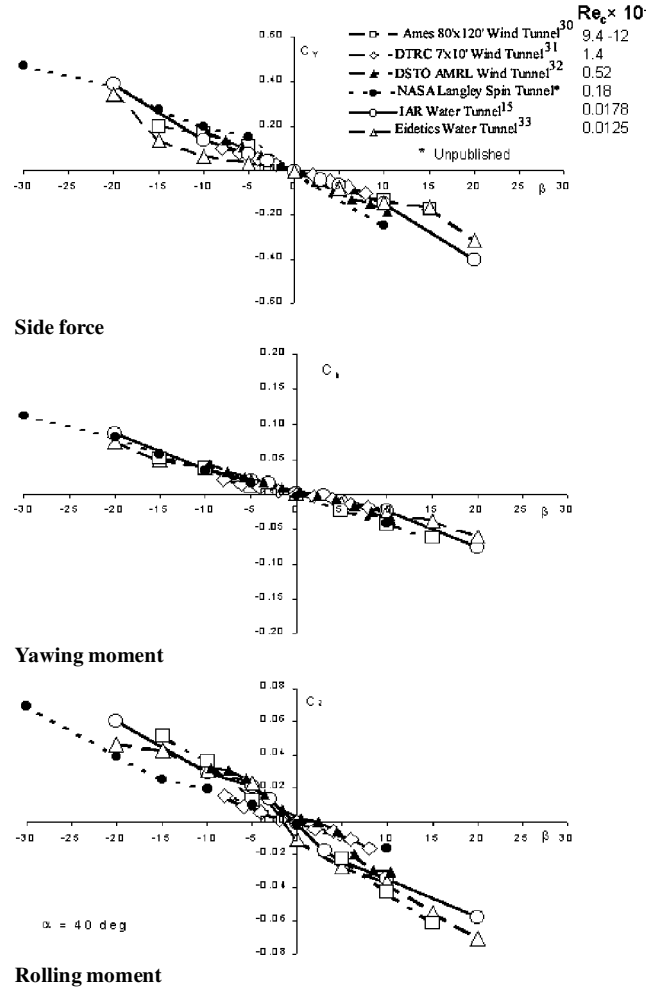

Fig. 21 Interfacility correlation of lateral–directional aerodynamics at $\alpha = 40$ deg.

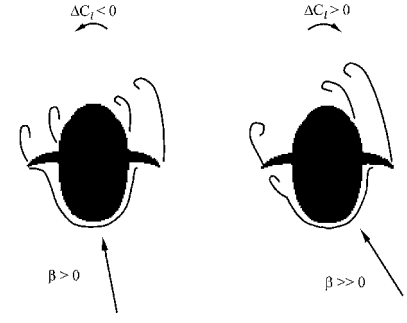

Fig. 22 Conceptual viscous fairing effects under laminar flow conditions at finite β.

numbers, as low as $M_\infty = 0.15$, have been attributed to compressibility effects.[57] These Mach number effects are caused by the high flow accelerations over the leading edge of the LEXs at high α. Compressibility effects on vortex breakdown could have played a role, but normally become significant only at higher subsonic Mach numbers. Because the forebody vortex strengths are essentially unaffected, the ratio of LEX-vortex to forebody-vortex strengths in-flight at $0.2 < M_\infty < 0.4$ is reduced in comparison to its incompressible water-tunnel counterpart. Thus, the reduction in LEX vortex lift due to the viscous-fairing-induced sweep angle increase tends to compensate for the lack of compressibility effects in the water tunnel.

Wing Leading-Edge Flaps

Whereas the forebody/LEX interactions are relatively insensitive to scale effects as a result of these compensating mechanisms, the reattaching flow on the inboard wing and leading-edge flap sections is expected to be sensitive to Reynolds number. Both flight tests of HARV[20] and surface flow visualization at $U_\infty = 20$ m/s using tufts at the Aeronautical and Maritime Research Laboratory (AMRL) in Australia[32] (Fig. 24) show regions of attached flow on the inboard section of the leading-edge flap. At $\alpha = 30$ deg and $\beta = 0$, the regions of attached flow on the leading-edge flap are small, and there is only a hint of a separation bubble. At $\alpha = 35$ deg and $\beta = 0$, there are small regions of attached flow on the leading-edge flap and a separation bubble of limited extent. In contrast, at $\alpha = 35$ deg and $\beta = \pm 10$ deg, the attached flow region on the leeward leading-edge flap and wing leading-edge vortex extended outboard along a substantial portion of the leading edge. Separation bubbles existed with reattachment on the leeward leading-edge flap. The nature of the separation bubble was defined by smoke flow visualization[32] at $\alpha = 40$ deg and $\beta = -10$ deg (Fig. 25). These results indicate that in the α range of interest, $30 \le \alpha \le 55$ deg, there is a β envelope beyond which Reynolds number effects could be significant.

In the unsteady case, validation of water tunnel results is challenging; no F/A-18 flight-test data are available, for instance, for a loaded roll maneuver. Nevertheless, the degree of similarity between laminar wind-tunnel and flight-test wing rock characteristics at $0.2 < M_\infty < 0.4$ (Fig. 18) constitutes an overall validation of the laminar to fully turbulent similarity concept.

Analysis and Consolidation of Database

Comparisons were made of the OPLEC water-tunnel data[15] in the α range from 25 to 90 deg with unpublished rotary balance data from the NASA Langley Research Center Spin Tunnel and with

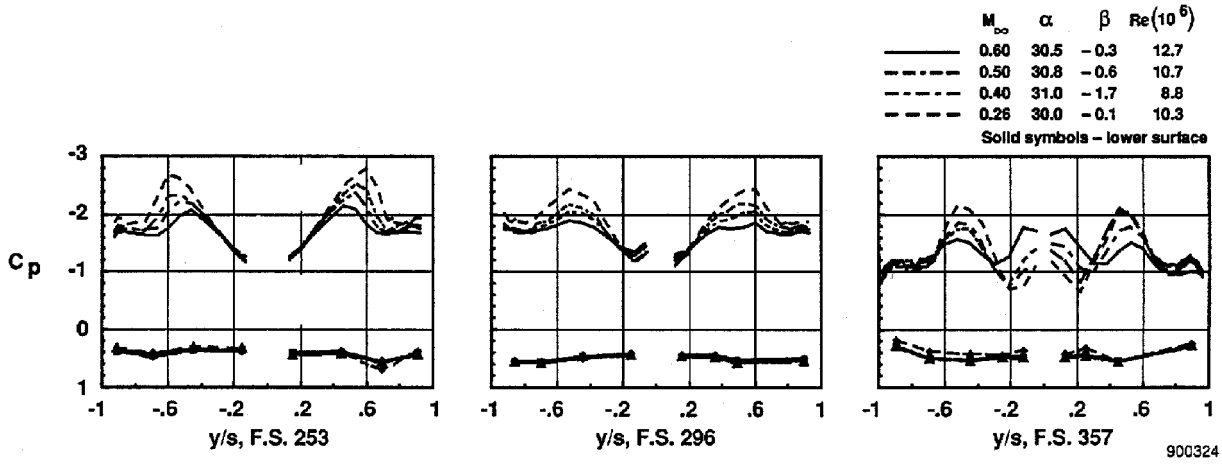

Fig. 23 Compressibility effect on LEX surface pressure coefficients on F/A-18 HARV[55] at $\alpha \cong 31$ deg.

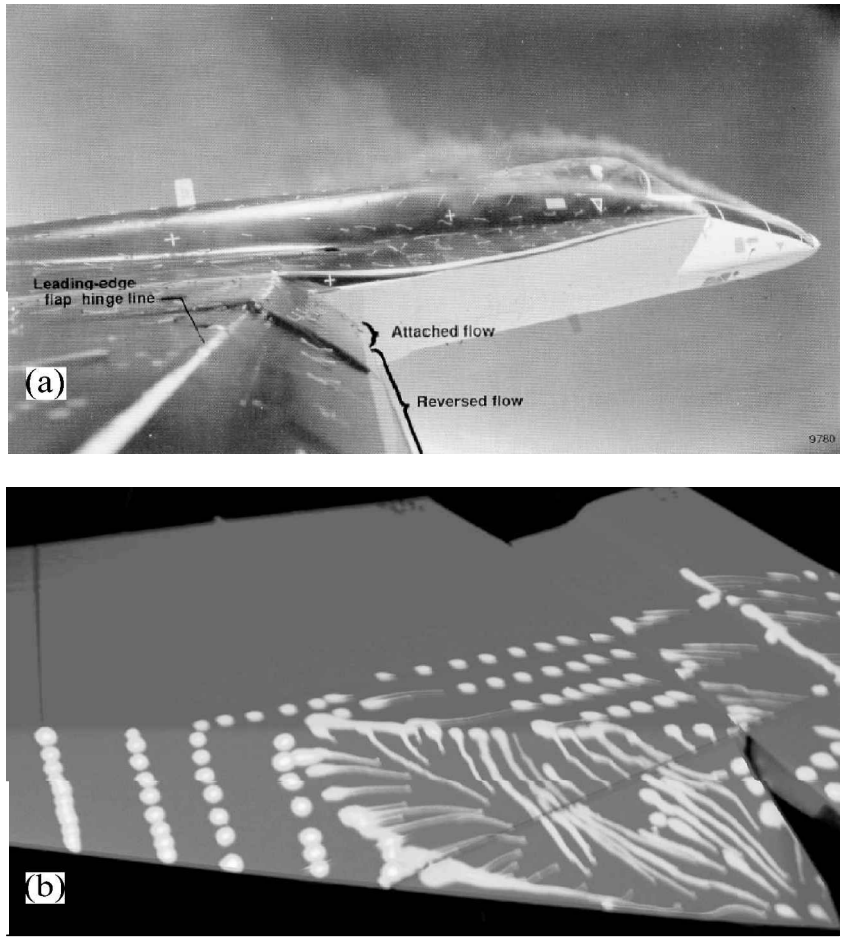

Fig. 24 Comparison of flow visualization on a) F/A-18 HARV using tufts[20] with b) dot-streak results[32] at $\alpha = 30$ deg.

results from other sources.[11,28] The comparison in Fig. 26 shows good agreement at $\alpha = 45$ deg for the side force C_Y and yawing moment C_n, but significant discrepancies in C_l between the three sets of wind-tunnel data. The IAR data and unpublished NASA Langley Research Center data at 45 deg agree reasonably well at large $\bar{\Omega}$, $|\bar{\Omega}| > 0.1$, but show quite different slopes at low $\bar{\Omega}$. It was pointed out[17] that this test was in the α range of susceptibility to support interference; it is also known that there is considerable sensitivity to Reynolds number and geometric variations between model and full scale. Effects of support interference were also evident in the NASA Langley Research Center C_l data at $\beta \neq 0$ and $\alpha \geq 40$ deg (Ref. 18).

The introduction of aerodynamic similarity parameters[6] has shown that considerable simplification of the F/A-18 nonplanar aerodynamics is possible in the domain of forebody/LEX vortex interactions, which is characterized by a dominant fluid/motion coupling mechanism. Good correlations were obtained between the lateral–directional aerodynamic characteristics from different degrees of freedom using parameters based on the effective differential sweep angles at the LEX apex, $\Lambda_{Z\,\mathrm{LEX}}$, at the nose tip, Λ_{Zn}, and the reduced body-axis yaw rate $\bar{r} = rb/2U_\infty$, in coning and steady sideslip. These parameters are derived from a dynamic crossflow parameter. For instance, analyzing the NASA Langley Research Center database it is found that at moderately high α the static

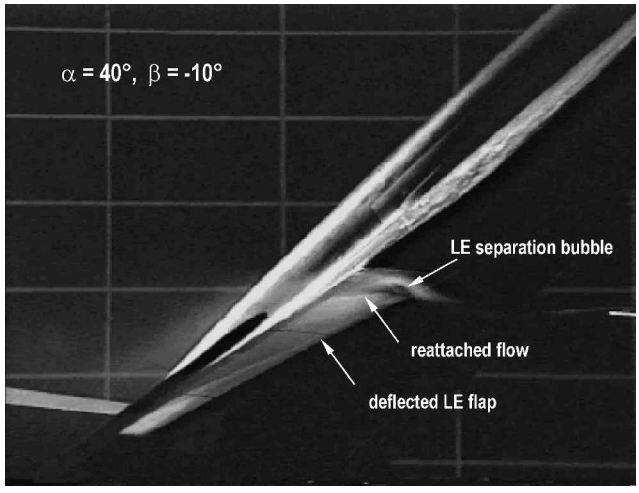

Fig. 25 Smoke flow visualization on leading-edge flap of 1/9-scale F/A-18 model.[32]

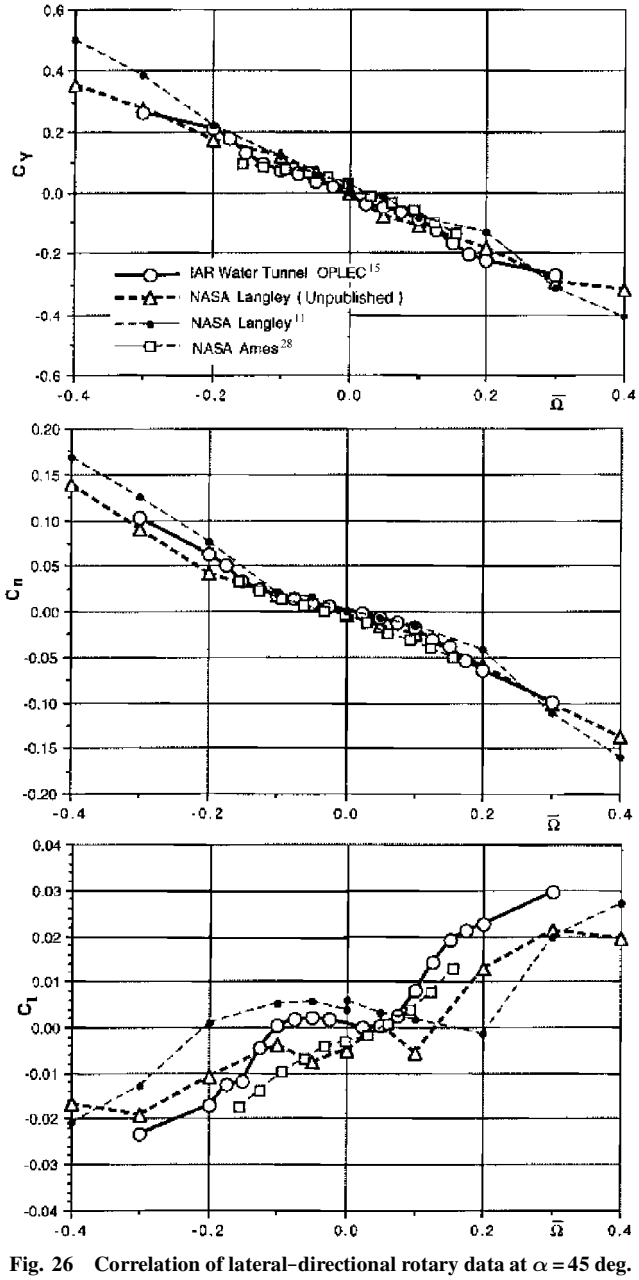

Fig. 26 Correlation of lateral–directional rotary data at $\alpha = 45$ deg.

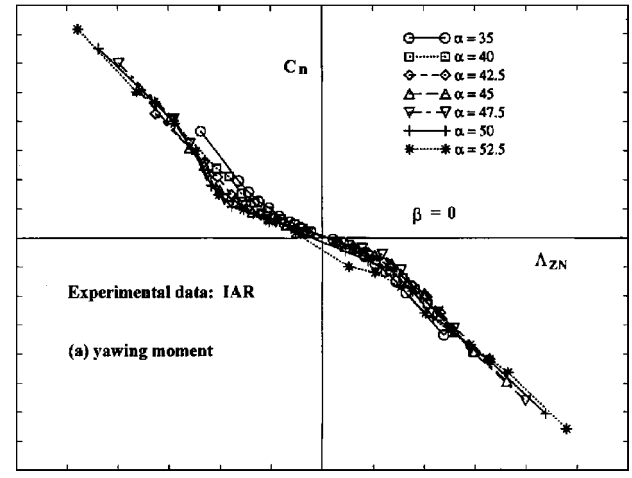

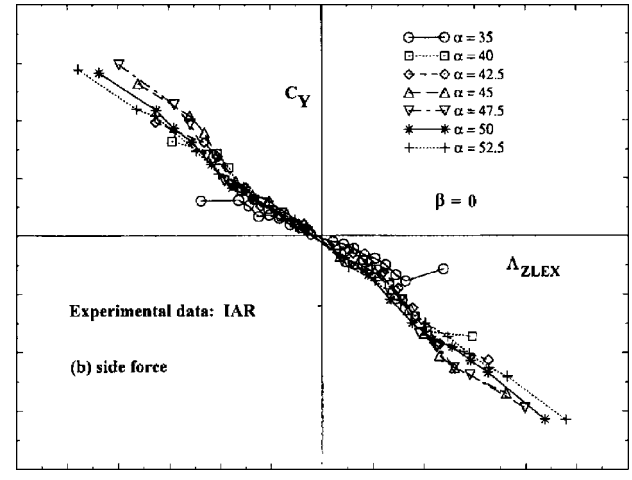

Fig. 27 Correlation of rotary aerodynamic data[15] at discrete angles of attack.[6]

and rotary C_n and C_Y data correlate well with Λ_{Zn} and Λ_{ZLEX}, as appropriate. As can be seen from the IAR data[6] in Figs. 27a and 27b, the results collapse to a single curve in each case. Both the $C_n(\Lambda_{Zn})$ and $C_Y(\Lambda_{ZLEX})$ characteristics at different values of β are well correlated for Λ_Z values of interest, when using these similarity parameters over the range $35 \leq \alpha \leq 52.5$ deg and $|\beta| < 30$ deg (Fig. 28).

Unlike the side force and yawing moment, the rolling moment at high α is dominated by the aerodynamic loading on the windward surfaces. C_l correlates well with $\bar{r}$ for $\alpha \geq \delta_{LE}$ at all β, up to a maximum rotation rate $\bar{r}_{max} \cong 0.2$, when the aerodynamic roll angle ϕ opposes the spin rate.[6] At these conditions, vortex breakdown is roughly symmetrical, and C_l is generated mainly by the windward aerodynamic loading. For rotation in the other direction, the differential loading due to asymmetric flow separation dominates, and the rolling moment increments increase monotonically with α. The similarity relationships for C_l are still being investigated. The analysis also facilitates the incorporation of engine inlet flow effects on vortex breakdown determined in a water tunnel.[35] To obtain the engine inlet flow effects on the rotary aerodynamics, the vortex breakdown data are correlated with a nonplanar similarity parameter that can be expressed in terms of Λ_Z.

No significant steady-state hysteresis was found within the vortex interaction range,[17] indicating that the use of similarity parameters was legitimate. Once the aerodynamic responses become discontinuous and steady-state bifurcation occurs, it is no longer possible to define a similarity parameter based on kinematic relationships alone. When natural asymmetric crossflow separation occurs on the forebody (at $\alpha \geq 57.5$ deg when $\beta = 0$ and at lower α at $\beta \neq 0$, depending on β and $\bar{\Omega}$) steady-state hysteresis occurs, and microasymmetry

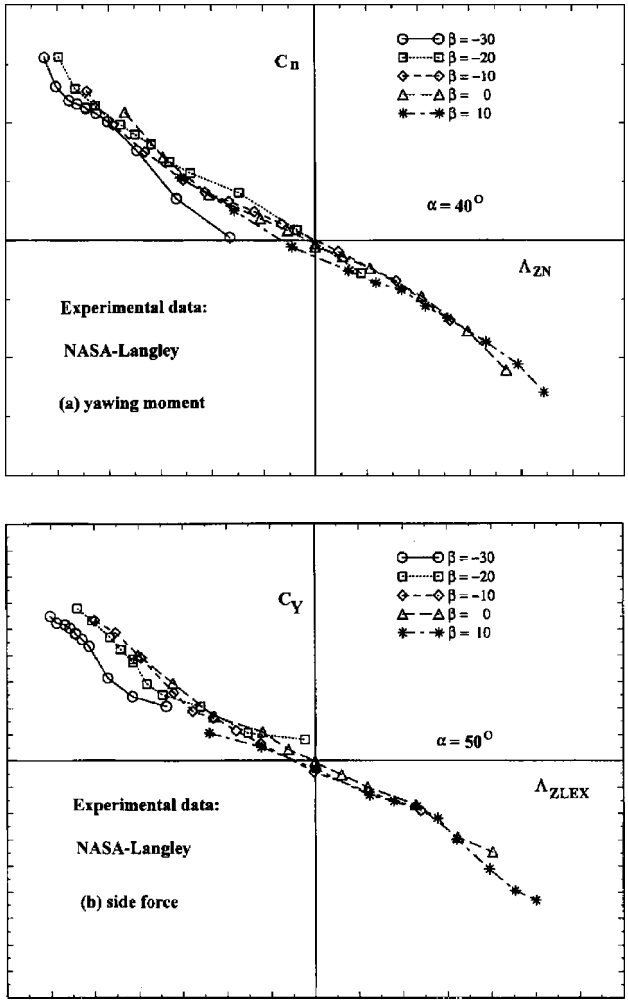

Fig. 28 Correlation of unpublished NASA Langley Research Center rotary data at discrete angles of sideslip.[6]

effects can play a large role. When using plastic kit models in water-tunnel tests, subtle variations in nose radius and concentricity and the presence of dye-flow orifices can have a significant effect on the angle of attack for onset of asymmetric vortex shedding. To avoid the latter problem in the IAR tests, different models were used for balance measurements and flow visualization, and the forebody nose cross section was checked.[15–17] Note that, in general, it is very difficult to simulate small-scale features or imperfections on full scale aircraft at model scale.[58] Moreover, different types of departure behavior can be exhibited from one aircraft to the next in the fleet.[22] When the experience of high-alpha aerodynamics of slender bodies of revolution[24] is drawn from, slight geometric changes in the model nose bluntness can be used to generate alternative data sets that model the different types of behavior representative of the specific aircraft studied. The correlation of rotary data at $\alpha = 60$ deg and $\beta = 0$ (Fig. 29) illustrates the different types of behavior, attributed to different model microasymmetries, to differences in test procedures, and to test Reynolds numbers.[6]

Poststall Flight Prediction

The conceptual steady-state bifurcation boundaries are illustrated in Fig. 30. Within the vortex interaction domain and the three-dimensional stall domain, analytic representations or two-dimensional table lookup and interpolation can be used for the lateral–directional data, with the possible exception of the proconing C_l data.[6] This representation allows the implementation of a modified quasi-steady model that circumvents many of the drawbacks of conventional 6-DOF models.[6] An example of the data used to de-

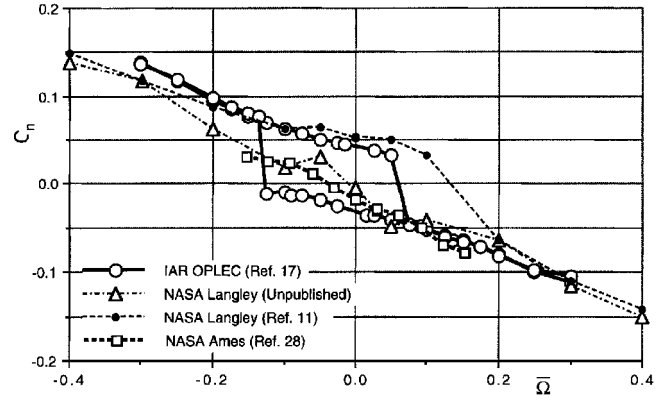

Fig. 29 Interfacility correlation of F/A-18 yawing moment at $\alpha = 60$ deg.

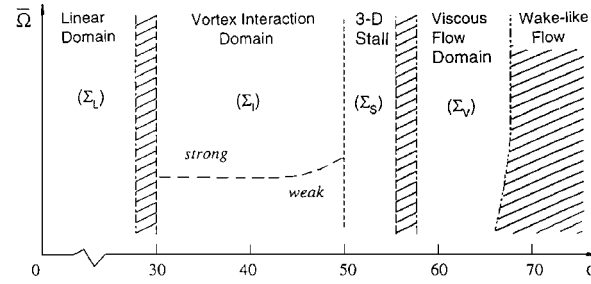

Fig. 30 Schematic steady-state bifurcation boundaries.

termine the steady-state bifurcation boundaries is shown in Fig. 11. The regions of unsteady flow at low $\bar{\Omega}$ are indicative of viscous interactions occurring at the low Reynolds number water-tunnel conditions. No wind-tunnel rotary data exist at these nonplanar conditions. Further tests at higher subcritical Reynolds number could conceivably clarify the sensitivity to small ϕ and $\bar{\Omega}$. Similar maps of the forebody/LEX vortex interaction conditions were generated at discrete ϕ values, defining the behavior beyond this range of unsteadiness. Finally, a separate map locates the approximate upper limit of reattaching flow on the wing/flap system. The flow physics considerations that account for the general laminar/fully turbulent data equivalence[9] and define the steady-state bifurcation boundaries that restrict the database also provide the rationale for applying the water tunnel data to simulate full-scale conditions. This validated water-tunnel database can be incorporated into flight simulator software.

For practical reasons, the bulk of the database will be obtained at subcritical Reynolds numbers. As has been pointed out,[9] unsteady aerodynamics at high Reynolds number conditions, in general, cannot be simulated by the use of boundary-layer trips at subcritical or critical conditions. However, there is a qualitative similarity between the unsteady aerodynamic responses in laminar and fully turbulent conditions.[9] Where a similarity does exist between the aerodynamics in subscale tests and low Mach number flight, the water tunnel is a convenient facility to generate the poststall nonplanar database, and there is some promise of simplified nonlinear modeling.[6] A corollary to this is that the critical Reynolds number boundary is not crossed during the simulated maneuver. In the viscous flow domain, where the dominance of the LEX-induced upwash is lost, the complexity increases greatly because Reynolds number effects, viscous fluid/motion coupling,[39] and microasymmetry effects dictate the time-dependent responses.

Conclusions

From a poststall simulator enhancement study, it became evident that in the case of the F/A-18 much of the required dynamic data applicable to flight at low Mach numbers could be generated in a water tunnel. The following conclusions may be drawn.

1) The water tunnel rotary investigation has generated a substantial addition to the F/A-18 poststall nonplanar database.

2) Flow physics analysis of the F/A-18 has provided a rationale for extrapolation of water-tunnel dynamic data to full scale, identifying the conditions under which there exist compensating effects of viscous- and compressibility-dominated flow mechanisms. This phenomenon accounts for the relative insensitivity of LEX vortex breakdown to Reynolds number at low Mach numbers.

3) Within the boundaries of applicability of the water-tunnel data, poststall aerodynamic results obtained under laminar flow conditions are reasonably representative of full-scale conditions, in spite of the fact that neither the Reynolds number nor the Mach number are simulated in the water tunnel.

4) In the vortex interaction domain, where similarity relationships have been established between associated lateral degrees of freedom, the domain of applicability of the water-tunnel rotary data can be clearly defined.

5) The introduction of nonplanar aerodynamic simulation parameters made possible the consolidation of results from diverse experimental sources, including static and rotary balance force measurements and water-tunnel and full-scale flowfield measurements.

6) The favorable correlations obtained on the F/A-18 are due, in large part, to its unique forebody/LEX geometry. Nevertheless, it is felt that implementation of the methodologies described could provide the insight needed to extrapolate to flight conditions water-tunnel poststall data on other related aircraft configurations.

Acknowledgments

This project was funded in part by Defence Research and Development Canada. The author wishes to recognize the contribution of Capt. D. A. Baker, DTA 3-4-3, scientific authority for the project. The author is grateful for the cooperation of David F. Fisher, NASA Dryden Flight Research Center, and Neil O'Connor, Bihrle Applied Research, Inc., in providing unpublished experimental data. The author also wishes to express appreciation to Hui-Juan Cai for her support (F/A-18 experiments and graphics). The author appreciates the valuable comments made by Lars Ericsson and David Fisher.

References

[1]"Use of Rotary Balance Data in the Prediction of Aircraft Dynamics," AGARD-AR-265, *Rotary Balance Testing for Aircraft Dynamics*, Dec. 1990, Chap. 9, pp. 188–208.8.

[2]Alcorn, C. W., Croom, M. A., and Francis, M. S., "The X-31 Experience: Aerodynamic Impediments to Post-Stall Agility," AIAA Paper 95-0362, Jan. 1995.

[3]Beyers, M. E., "Interpretation of Experimental High-Alpha Aerodynamics: Implications for Flight Prediction," *Journal of Aircraft*, Vol. 32, No. 2, 1995, pp. 247–261.

[4]"CF-18A/CF-18B Hornet Aircraft Operating Instructions (English)," National Defence Index of Documentation C-12-188-NFM/MB-001, Modification 1, Canadian Dept. of National Defence, Ottawa, Jan. 2002.

[5]Hall, R. M., Banks, D. W., Fisher, D. F., Ghaffari, F., Murri, D. G., and Ross, J. C., "A Status Report on High Alpha Technology Program (HATP) Ground Test to Flight Comparisons," NASA CP 10143, Vol. 1, July 1994.

[6]Beyers, M. E., "F/A-18 Nonplanar Maneuvering Aerodynamics," *Canadian Aeronautics and Space Journal*, Vol. 47, No. 2, 2001, pp. 57–69.

[7]Ericsson, L. E., "Reflections Regarding Recent Rotary Rig Results," *Journal of Aircraft*, Vol. 24, No. 1, 1987, pp. 25–30.

[8]Ericsson, L. E., and Beyers, M. E., "Aspects of Ground Facility Interference on Leading-Edge Vortex Breakdown," *Journal of Aircraft*, Vol. 38, No. 2, 2001, pp. 310–314.

[9]Ericsson, L. E., and Beyers, M. E., "Wind-Tunnel Aerodynamics in Rotary Tests of Combat Aircraft Models," *Journal of Aircraft*, Vol. 35, No. 4, 1998, pp. 521–528.

[10]Polhamus, E. C., "A Review of some Reynolds Number Effects Related to Bodies at High Angles of Attack," NASA CR-3809, Aug. 1984.

[11]Hultberg, R., "Low Speed Rotary Aerodynamics of F-18 Configuration for 0 to 90 Angle of Attack—Test Results and Analysis," NASA CR 3608, Aug. 1984.

[12]Erickson, G. E., "Water Tunnel Flow Visualization and Wind Tunnel Data Analysis of the F/A-18," NASA CR-165859, May 1982.

[13]Beyers, M. E., "Orbital Platform Concept," *Future Concepts, Rotary Balance Testing for Aircraft Dynamics*, AGARD AR-265, Dec. 1990, Chap. 6.2.

[14]Beyers, M. E., "Unsteady Wind-Tunnel Interference in Aircraft Dynamic Experiments," *Journal of Aircraft*, Vol. 29, No. 6, 1992, pp. 1122–1129.

[15]Cai, H. J., and Beyers, M. E., "OPLEC Rotary Experiments on the F/A-18," National Research Council, Inst. for Aerospace Research, Rept. IAR LTR-A-021, Ottawa, ON, Canada, March 1998.

[16]Cai, H. J., and Beyers, M. E., "OPLEC Flow Visualization on F/A-18 at Zero Sideslip," National Research Council, Inst. for Aerospace Research, Rept. IAR LTR-A-42, Ottawa, ON, Canada, Aug. 1999.

[17]Cai, H. J., and Beyers, M. E., "OPLEC Investigation of F/A-18 High-Alpha Nonlinearities," National Research Council, Inst. for Aerospace Research, Rept. IAR LTR-A-046, Ottawa, Canada, March 2000.

[18]Beyers, M. E., and Cai, H. J., "F/A-18 Post-Stall Aerodynamic Database," National Research Council, Inst. for Aerospace Research, Rept. IAR LTR-AL-2001-0088, Ottawa, Canada, Dec. 2001.

[19]Fisher, D. F., Del Frate, J. H., and Zuniga, F. A., "Summary of In-Flight Flow Visualization Obtained from the NASA High Alpha Research Vehicle," NASA TM 101734, Jan. 1991.

[20]Fisher, D. F., Del Frate, J. H., and Richwine, D. M., "In-Flight Flow Visualization Csharacteristics of the NASA F-18 High Alpha Research Vehicle at High Angles of Attack," NASA TM-4193, May 1990.

[21]Quast, T., Nelson, R. C., and Fisher, D. F., "A Study of High Alpha Dynamics and Flow Visualization for a 2.5% Model of the F-18 HARV Undergoing Wing Rock." AIAA Paper 91-3267, Sept. 1991.

[22]Fisher, D. F., and Cobleigh, B. R., "Controlling Forebody Asymmetries in Flight—Experience with Boundary Layer Transition Strips," NASA TM 4595, July 1994.

[23]Hall, R. M., "Influence of Reynolds Number on Forebody Side Forces for 3.5-Diameter Tangent–Ogive Bodies," AIAA Paper 87-2274, Aug. 1987.

[24]Ericsson, L. E., and Reding, J. P., "Asymmetric Flow Separation and Vortex Shedding on Bodies of Revolution," edited by M. J. Hemsch, Vol. 141, Progress in Astronautics and Aeronautics, AIAA, Washington, DC, 1992, pp. 391–452.

[25]O'Connor, C. J., Ralston, J. N., and Fitzgerald, T., "Evaluation of the NAWC/AD F/A-18 C/D Simulation Including Database Coverage and Dynamic Data Implementation Techniques," AIAA Paper 96-3365, Aug. 1996.

[26]Greenwell, D. I., "Difficulties in the Application of Stability Derivatives to the Manoeuvring Aerodynamics of Combat Aircraft," International Council of the Aeronautical Sciences, Rept. ICAS-98-1.7.1, Melbourne, VIC, Australia, Sept. 1998.

[27]Hanff, E. S., and Jenkins, S. B., "Large-Amplitude High-Rate Roll Experiments on a Delta and Double Delta Wing," AIAA Paper 90-0224, Jan. 1990.

[28]Kramer, B. R., Suarez, C. J., Malcolm, G. N., and Ayers, B. F., "F/A-18 Forebody Vortex Control, Volume 2-Rotary-Balance Tests," NASA CR 4582, March 1994.

[29]Suarez, C. J., Malcolm, G. N., Kramer, B. R., Smith, B. C., and Ayers, B. F., "Development of a Multicomponent Force and Moment Balance for Water Tunnel Applications, Vol. 2," NASA CR 4642, Dec. 1994.

[30]Lanser, W. R., and Murri, D. G., "Wind Tunnel Measurements on a Full-Scale F/A-18 with Forebody Slot Blowing or Forebody Strakes," AIAA Paper 93-1018, Feb. 1993.

[31]Erickson, G. E., Hall, R. M., Banks, D. W., Del Frate, J. H., Schreiner, J. A., Hanley, R. J., and Pulley, C. T., "Experimental Investigation of the F/A-18 Vortex Flows at Subsonic Through Transonic Speeds," AIAA Paper 89-2222, Aug. 1989.

[32]Brian, G. J., Keating, H. A., and Quick, H. A., "Low-Speed Wind Tunnel Tests on a 1/9th Scale Model of the F/A-18 for a Range of Angles-of-Sideslip at High Angles-of-Attack," Defence Science and Technology Organisation, DSTO TN-M1/9/908, 2002.

[33]Suarez, C. J., Malcolm, G. N., Kramer, B. R., Smith, B. C., and Ayers, B. F., "Development of a Multicomponent Force and Moment Balance for Water Tunnel Applications, Vol. 1," NASA CR 4642, Dec. 1994.

[34]Del Frate, J. H., and Zuniga, F. A., "In-Flight flowfield Analysis on the NASA F-18 High Alpha Research Vehicle with Comparisons to Ground Facility Data," AIAA Paper 90-0231, Jan. 1990.

[35]Giacobello, M., and Drobik, J. S., "The Effect of Angle-of-Attack, Sideslip and Engine Inlet Flow on the Vortex Breakdown Over the F/A-18—A Water Tunnel Flow Visualisation Study," Defence Science and Technology Organisation, DSTO TN-M1/9/838, 2002.

[36]Wentz, W. H., "Vortex-Fin Interaction on a Fighter Aircraft," AIAA Paper 87-2474, Aug. 1987.

[37]Beyers, M. E., and Ericsson, L. E., "Extraction of Subscale Free-Flight Aerodynamics from Rotary Tests of Combat Aircraft," AIAA Paper 97-0730, Jan. 1997.

[38]Beyers, M. E., and Ericsson, L. E., "Implications of Recent Rotary Rig Results for Flight Prediction," *Journal of Aircraft*, Vol. 37, No. 4, 2000, pp. 545–553.

[39]Ericsson, L. E., and Beyers, M. E., "Universality of the Moving Wall Effect," *Journal of Aircraft*, Vol. 37, No. 2, 2000, pp. 508–513.

[40]Beyers, M. E., and Ericsson, L. E., "Why is LEX Vortex Breakdown on the F/A-18 Configuration Insensitive to Reynolds Number?," AIAA Paper 2001-0690, Jan. 2001.

[41]Hedley, J. W., "Analysis of Wind Tunnel Data Pertaining to High Angle of Attack Aerodynamics. Vol. 1—Technical Discussion and Analysis of Results," U.S. Air Force Flight Dynamics Lab., Dayton, OH, AFFDL-TR-78-4, July 1978.

[42]Wentz, W. H., and Kohlman, D. L., "Vortex Breakdown on Slender Sharp-Edged Wings," *Journal of Aircraft*, Vol. 8, No. 3, 1971, pp. 156–161.

[43]Lamar, J. E., and Frink, N. T., "Experimental and Analytical Study of the Longitudinal Aerodynamic Characteristics of Analytically and Empirically Designed Strake-Wing Configurations at Subcritical Speeds," NASA TP 1803, June 1981.

[44]Straka, W. A., and Hemsch, M. J., "Effect of a Fuselage on Delta Wing Vortex Breakdown," *Journal of Aircraft*, Vol. 31, No. 4, 1994, pp. 1002–1005.

[45]Ericsson, L. E., "Comment on 'Effect of a Fuselage on Delta Wing Vortex Breakdown," *Journal of Aircraft*, Vol. 31, No. 4, 1994, pp. 1006–1007.

[46]Ericsson, L. E., "Further Analysis of Fuselage Effects on Delta Wing Aerodynamics," AIAA Paper 2000-0981, Jan. 2000.

[47]Ericsson, L. E., and Beyers, M. E., "Aspects of Ground Facility Interference on Leading-Edge Vortex Breakdown," AIAA Paper 2000-0978, Jan. 2000.

[48]Earnshaw, P. P., "Measurements of Vortex-Breakdown Position at Low Speed on a Series of Sharp-Edged Symmetrical Models," Aeronautical Research Council, London, U.K., CP 828, Nov. 1964.

[49]Ericsson, L. E., "Separated Flow Mechanisms in F-18 Wing Rock," *Journal of Aircraft*, Vol. 33, No. 1, 1996, pp. 81–86.

[50]Thompson, D. H., "A Visualization Study of the Vortex Flow around Double-Delta Wings," Aeronautical Research Labs., Rept. ARL-AERO-R-165, Melbourne, VIC, Australia, Aug. 1985.

[51]Verhaagen, N. G., Jenkins, L. N., Kern, S. B., and Washburn, A. E., "A Study of the Vortex Flow over a 76/40 Double-Delta Wing," AIAA Paper 95-0650, Jan. 1995.

[52]Fritzelas, A. E., Platzer, M. F., and Hebbar, S. K., "Effect of Reynolds Number on High-Incidence Flow over Double-Delta Wings," AIAA Paper 97-0046, Jan. 1997.

[53]Bergmann, A., Hummel, D., and Oelker, H.-C., "Vortex Formation over a Close-Coupled Canard-Wing-Body Configuration in Unsymmetrical Flow," AGARD-CP-494, Vortex Flow Aerodynamics: papers presented and discussions from the Fluid Dynamics Panel Symposium in Scheveningen, The Netherlands, AGARD, Neuilly-sur-Seine, France, 1991, pp. 14-1–14-14.

[54]Hemsch, M. J., and Luckring, J. M., "Connection Between Leading-Edge Sweep, Vortex Lift, and Vortex Strength for Delta Wings," *Journal of Aircraft*, Vol. 27, No. 5, 1990, pp. 473–475.

[55]Fisher, D. F., Banks, D. W., and Richwine, D. M., "F-18 High Alpha Research Vehicle Surface Pressures: Initial In-Flight Results and Correlation with Flow Visualization and Wind Tunnel Data," NASA TM 101724, Aug. 1990.

[56]Banks, D. W., Fisher, D. F., Hall, R. M., Erickson, G. E., Murri, D. G., Grafton, S. B., and Sewall, W. G., "The F/A-18 High-Angle-of-Attack Ground-to-Flight Correlation: Lessons Learned," NASA TM 4783, Jan. 1997.

[57]Kramer, B. R., Malcolm, G. N., Suarez, C. J., and James, K. D., "Pressure Distributions Around an F/A-18, in Static and Rotary Flow Fields, with Forebody Vortex Control," AIAA Paper 94-1828, Aug. 1994.

[58]Skow, A. M., "Comment in Round Table Discussion," AGARD-CP-247, High Angle of Attack Aerodynamics: papers presented and discussions from the Fluid Dynamics Panel Symposium in Sandefjord, Norway, AGARD, Neuilly-sur-Seine, France, 1979, pp. RTD-3–RTD-4.